

THE ELECTRON BEAM DYNAMICS IN ELECTRON COOLER ERL FOR RHIC.

I.	About this document	2
II.	The RHIC e-cooler facility	2
III.	Electron Beam Parameters	2
IV.	General ERL layout	3
IV.A.	Two loops magnetic system.....	4
V.	Transport line to RHIC	6
V.A.	Matching two rings	6
V.B.	The undulator matched beta function.....	8
VI.	Super conductive RF photo injector.....	9
VI.A.	SC RF Gun	9
VI.B.	Merger system.....	11
VI.B.1.	Achromatic merger at present of a strong space charge effects	11
VI.B.2.	Beam dynamic for different initial laser shape.....	14
VI.B.3.	Sensitivity to driving laser beam parameters.....	17
VII.	Start-to-end simulation.....	18
VIII.	Super conductive linac	19
IX.	Beam break up instability	21
	REFERENCES.....	21

I. About this document

The purpose of this document is to give a brief introduction in some beam dynamics aspects in electron cooling facility for Relativistic Heavy Ion Collider based on energy recovery linac (ERL). Many sections will be added in this short document soon.

II. The RHIC e-cooler facility

The project of 10-fold increasing RHIC luminosity using high energy electron cooling for is under developed now in Brookhaven National Laboratory [1].

In present project a single ERL will provide electron beam for electron cooling both rings simultaniosly. An electron cooling will be applied to both yellow and blue RHIC rings at 2 o'clock interaction point. The site plan of the RHIC electron cooler facility is shown on the Figure II-1.

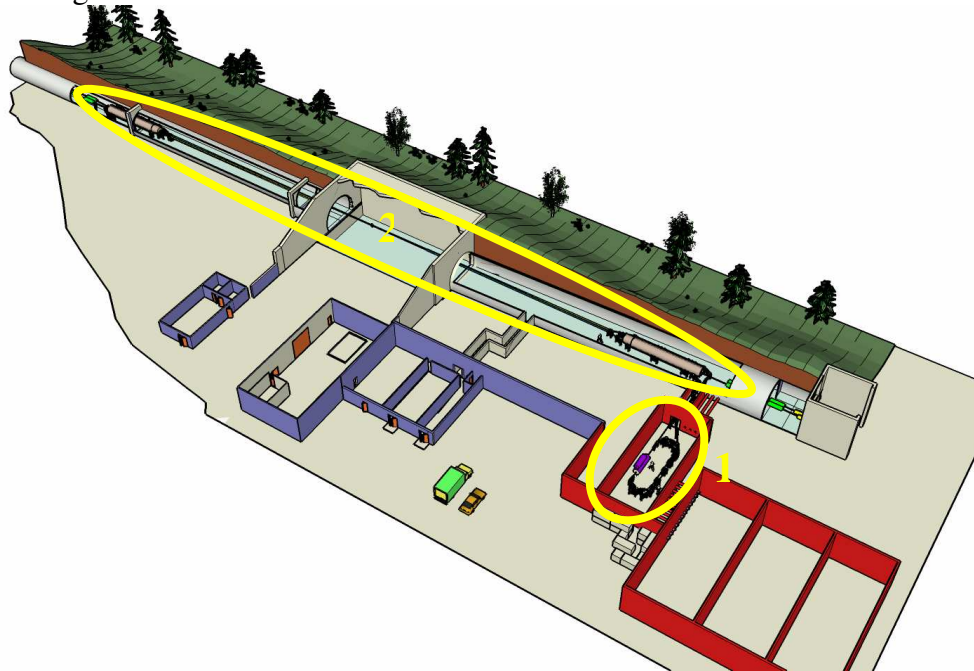


Figure II-1. A 3D Site view of the RHIC electron cooler.

The electron cooler facility consists of the two main components: an ERL (1) in order to provide the electron beam, and a cooling section (2) to interact ion- with electron- beams.

III. Electron Beam Parameters

The electron beam parameters required to provide sufficient RHIC gold beams cooling rate is shown in the Table III-1.

Table III-1. Required electron beam parameters

Kinetic energy , MeV	54.34
Charge per bunch, nC	5

Rms normalized emittance, mm·mrad	4
Rms bunch radius, mm	4.3
Beta function in the cooler section, m	500
Rms momentum spread	$3 \cdot 10^{-4}$
Rms bunch length, cm	1
Repetition rate, MHz	9.383
Average current, mA	47
Relativistic factor γ	107.35

IV. General ERL layout

The schematic layout two passes e-cooler ERL is shown on Figure IV-1.

The superconducting RF (SRF) Gun (1) produces 5 nC 4.7 MeV electron beam. The beam goes through the injection channel (2) comes into SC RF Linac (3) to be accelerated first time up to 30 MeV. The 30 MeV beam makes two achromatic 180 degrees bends (4, 4') and come back in to the linac (3) second time to get acceleration to 54.5 MeV. The 54.5 is transported to the RHIC (5) for cooling ion beam in both rings (see VII). The used 54.5 MeV electron beam is returning back (6) into the linac (3) in decelerated phase. After first deceleration to 30 MeV beam goes through two 180 degrees achromatic bends (4,4') again. In the last time passing through the linac beam gives back rest of the energy to cavities and goes to beam dump (7) having injection energy 4.7 MeV.

The decelerating beams deposit into the SRF linac the same amount of energy as that take by accelerating beams. Therefore, the RF power required to operate the SRF linac is very low and is at few watts level. We are going to use of the 50 kW RF transmitter for operating SRF linac is required mostly to compensate for reactive power load caused by micro-phonics.

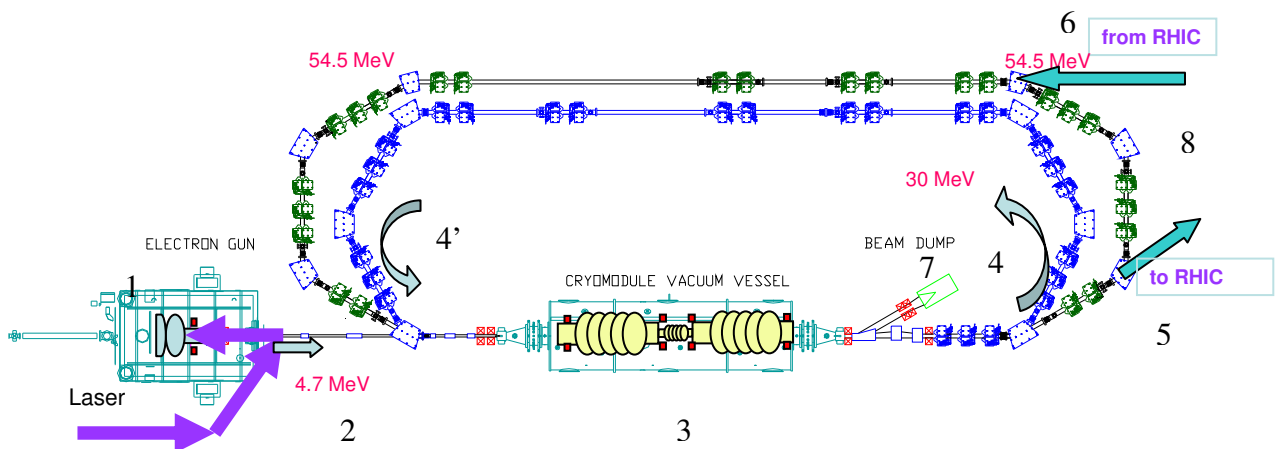


Figure IV-1. Schematic layout of two passes ERL for the RHIC electron cooler facility: 1) SC RF gun, 2) injection channel, 3) SC RF linac, 4) and 4') 180 degrees

achromatic bends, 5) and 6) transport channels to- and from- RHIC, 7) beam dump, 8) short-cut.

IV.A. Two loops magnetic system

Each 180 degrees bends of the first loop (4) and (4') consists from three 60 degrees dipole magnets (Fig.IV-A-1-a) with three independent quadrupole magnets (Fig.IV-A-1-b) between them. The quadrupoles between the dipoles makes the bends achromatic and isochronous. Nine quadrupoles in the dispersion-free straight section provides for matching of the β -function and for choosing the desirable phase advances independently in horizontal and vertical planes. At relatively high energy 30 MeV space charge effects to beam dynamics become very small. In first approximation a linear matrix approach can be used for layout design and matching electron beam from linac with returning loop. The MAD output lattice functions for first pass from linac exit to next entrance to the linac are shown on Fig. IV-A-2.

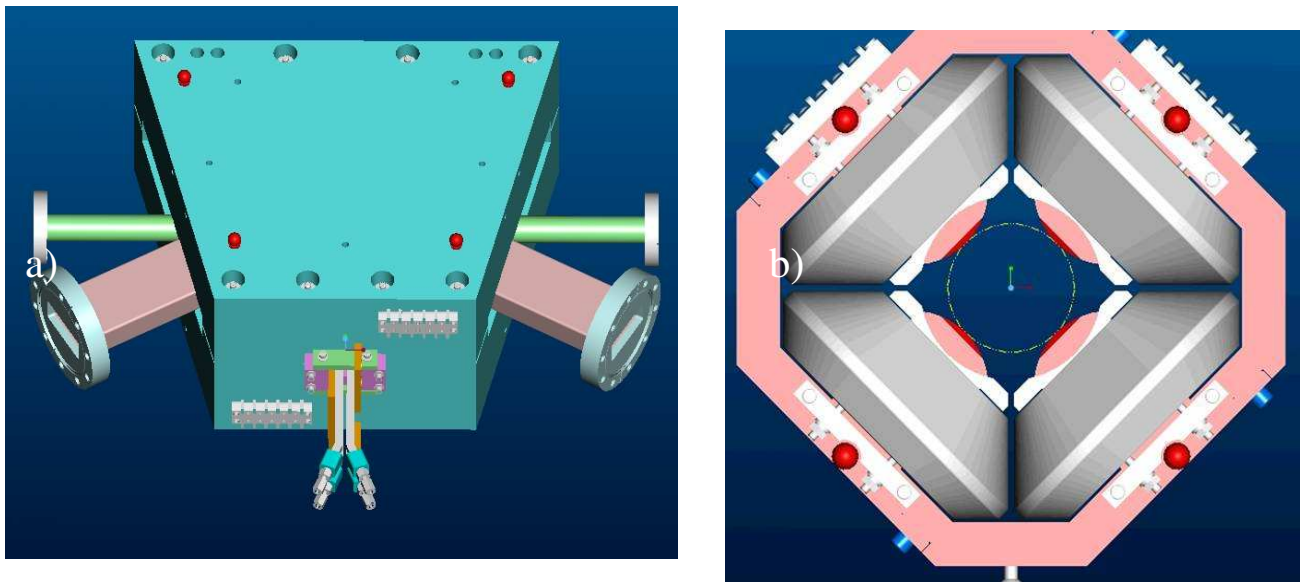


Figure IV.A-1. The magnets of the first loop assembly: a) 60 degrees chevron dipole magnet, b) 5 cm ID quadrupole magnet.

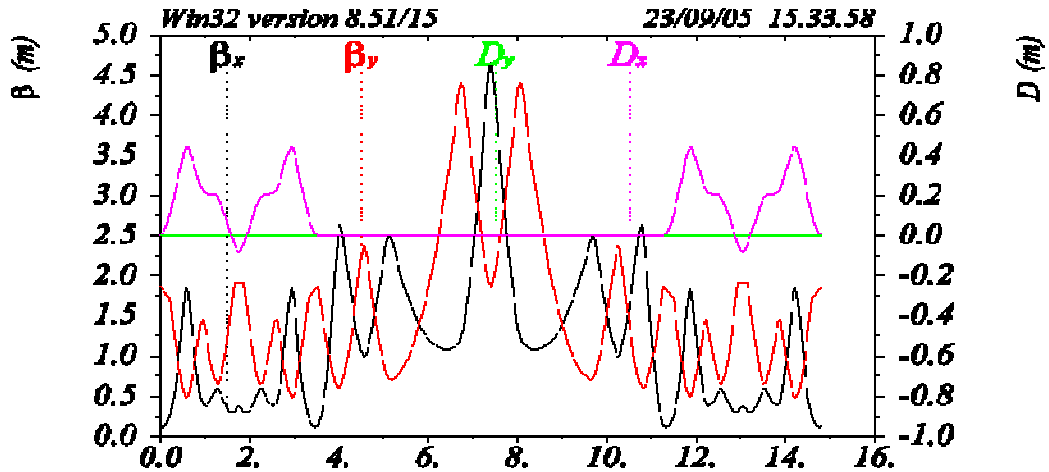


Figure IV.A-2. The beta functions and dispersion evaluation in the first loop.

A dispersion in the bends is always smaller 0.5 m. There is dispersion free section between of two 180 degrees bends. A zero longitudinal dispersion of the whole loop makes the longitudinal motion in first order very simple (see chapter X). The present design of second loop lattice has a short-cut (8) (Fig. IV-1) to drive electron beam directly to the linac in decelerating phase with out reaching cooling region. This short-cut will be used for independent tests of ERL it self without interfere in RHIC operation. Energy of electron beam at the second loop is 54.5 MeV and effects of the space charge can be neglected even more. The lattice functions for second loop from linac exit at 54.3 MeV energy to entrance in decelerating phase to the linac again are shown on Fig. IV.A-3.

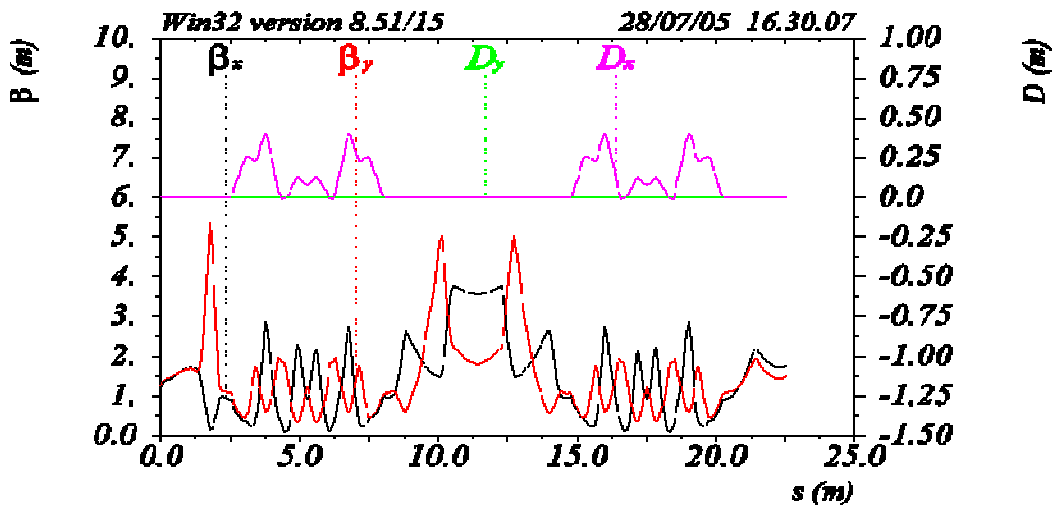


Figure IV.A-3. The beta functions and dispersion evaluation in the second loop short-cut.

There is also dispersion free section between two 180 degrees bends where beam will be studied more accurately before sending to RHIC.

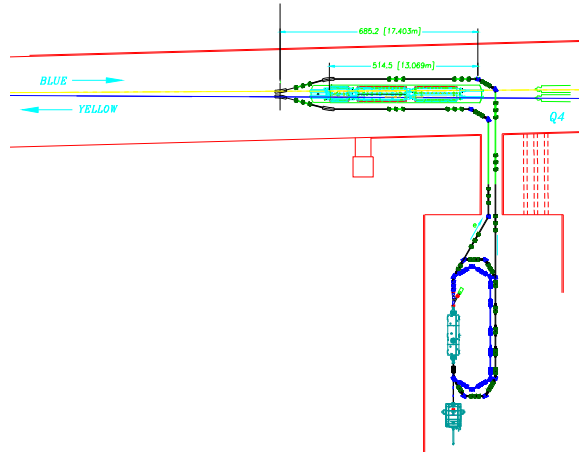


Figure IV.A-4. Layout of transport line from ERL to RHIC and back.

V. Transport line to RHIC

After reaching energy 55 MeV the electron beam follows to the RHIC. The transport line consists of similar quadrupoles and dipoles (Fig. IV. A-4). Magnet drive the electron beam to the RHIC and back. Quadrupoles provide matching beta functions from ERL and cooling section and make dispersion zero in cooling section.

V.A. Matching two rings

The studies of electron beam performance degradation after one pass through cooling section in one ring shows that emittance could grow less than 1 % [2]. The electron beam performances are still good enough to reuse such beam for cooling of other ring ion beam. To keep parameters of cooling the same the electron beam should be well matched between two rings. The transport line from one ring to other should satisfied following requirements:

- beta functions should be matched with beta functions in cooling sections 500 m (see Tab. III-1);
- full time from a center of the cooling section in one ring to a center of cooling section in other ring should be integral number of ion beams period $1/9.383 \text{ MHz} = 106.6 \text{ nsec}$.

The schematic layout of the two rings matcher is shown on Fig. V-1. The region there the matcher could be installed is limited by the sizes of RHIC tunnel and necessity to bypass of matching RHIC superconducting triplet. In present design the electron time trip from center of yellow ring to center of blue ring is 4 distances between bunches.

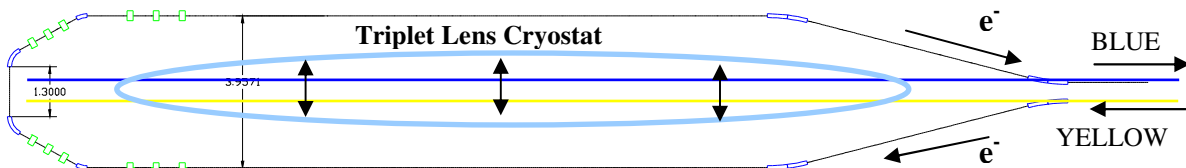


Figure V.A-1. Two ring achromatic matcher. Blue boxes are dipoles and green boxes are quadrupoles.

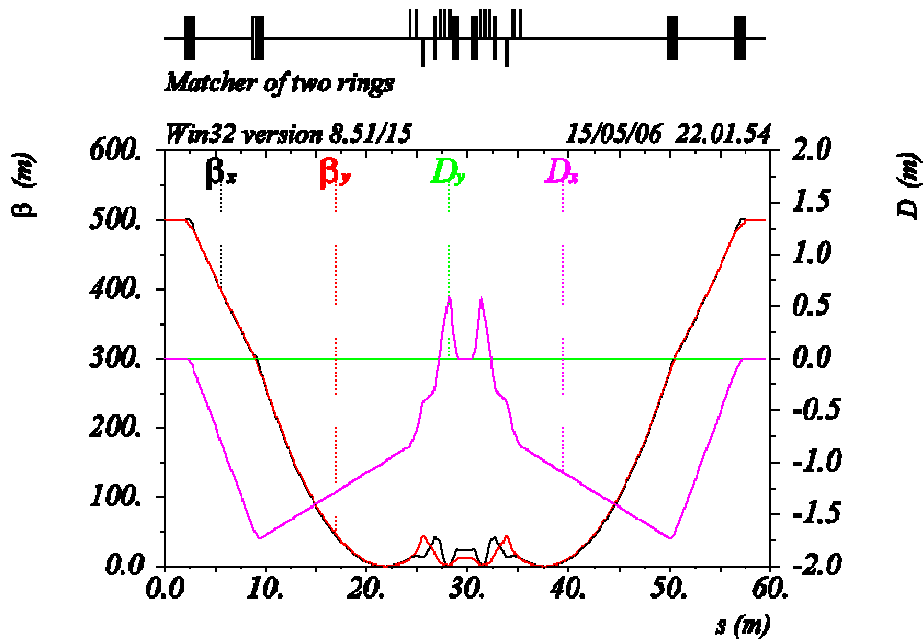


Figure V.A-2. Beta-function and dispersion in the matcher of two rings.

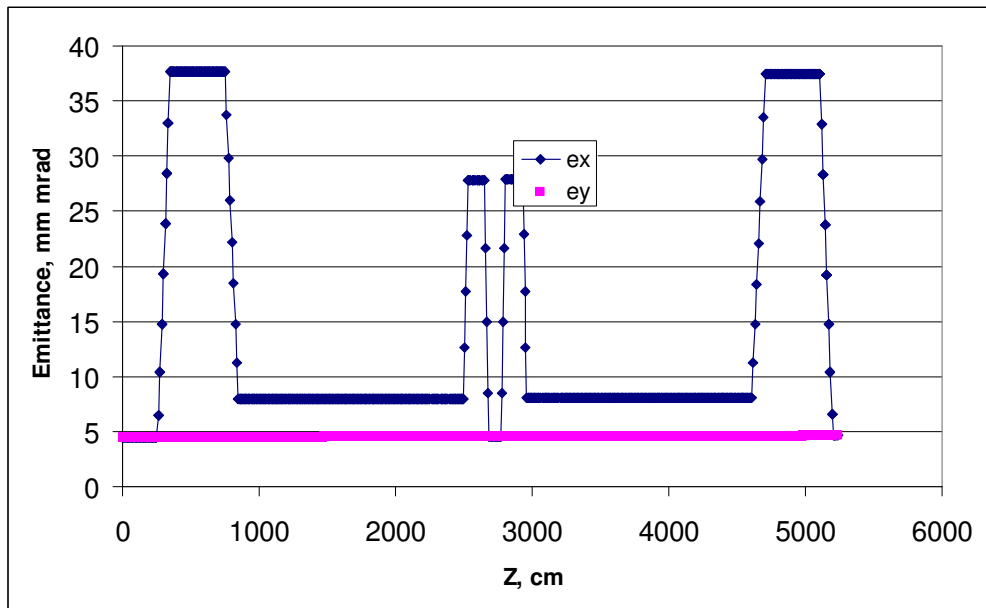


Figure V.A-3. Normalized emittances evaluations in the matcher of two rings.

The beta function in the rings is 500 m to avoid large beta function oscillations the weak chevron 15 degree 4 m radius dipoles input and output electron beam to and from ion beam trajectory. Before making 180 degree strong focusing turn the simple optics like telescope is used. The system has a zero dispersion region near an intersection of electron beam vacuum camera and RHIC vacuum camera. The beta function and dispersion are shown on Fig. V-2. To avoid vacuum cameras intersection the small vertical tilt of all electron beam trajectory can be used but in this case the vertical dispersion has to be taken to the account.

The effective horizontal emittance growth because of nonzero dispersion region is shown on Fig. V. A-3. However the emittance come back to normal numbers after beam come back to RHIC ring.

One of the interesting scenarios of the cooler running is to increase repetition rate of electron beams twice and chose the loop time instead of 4 distances between ion beams 3.5 distances. In this scenario odd numbers of electron beams will interact only with blue ring ions and the even number will interact only with yellow beam ions. The advantage of this each ring is cooled by fresh electron beam. The disadvantage is the avrage electron current grows twice.

V.B. The undulator matched beta function.

Using the undulator in cooling section was proposed in order to suppress effects of recombination. For suppressing effects of recombination in 10 times the 10 Gauss undulator field is needed [2].

There is formula for calculation matched beta function in helical undulator:

$\beta_0 = \sqrt{2} \frac{pc}{eB}$, where B magnetic field, p - electron beam avrage momentum, c - light velocity, e – electron charge and β_0 – matched beta-function.

In present design, electron beam has full energy 55 MeV and matched beta function is 260 m. The beta function of electron beam 500 m is mismatch and not a constant anymore see Fig. V.B-1. The ion beta function is also not a constant in drift space.

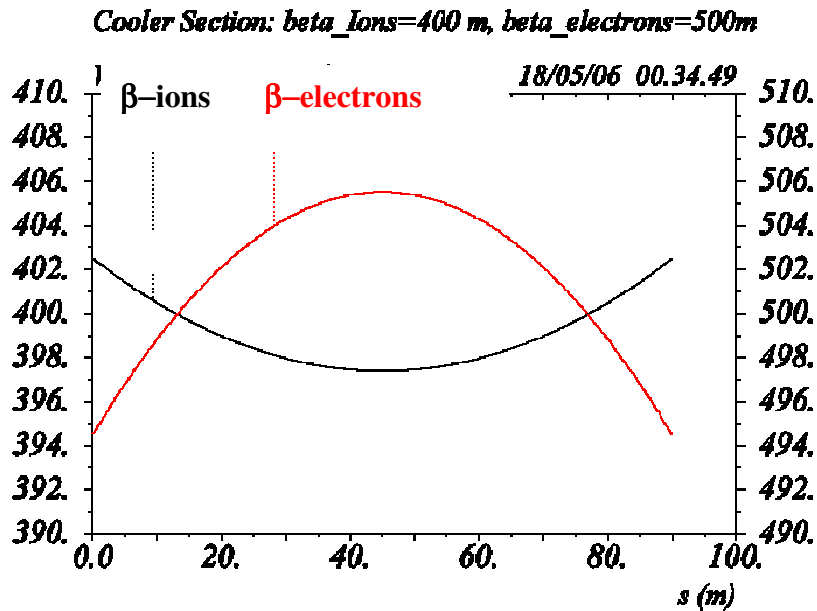


Figure V.B-1. Mismatched beta-functions: black – 400 m for ions, red – 500 m for electrons.

The maximum amplitude of deviation beta function of electrons from 500 m is +/- 6 m. For ions there is almost no focusing and beta function has a behavior like in a drift space, the maximum amplitude of deviation beta function of ions from 400 m is +/- 2.5 m.

VI. Super conductive RF photo injector

The electron cooler injector (see Fig. VI-1) consist of 1 ½ superconducting RF gun, solenoid, four chevron dipoles (split focusing) and two solenoids turned on in opposite direction (in order to match the electron beam with linac entrance more accurately).

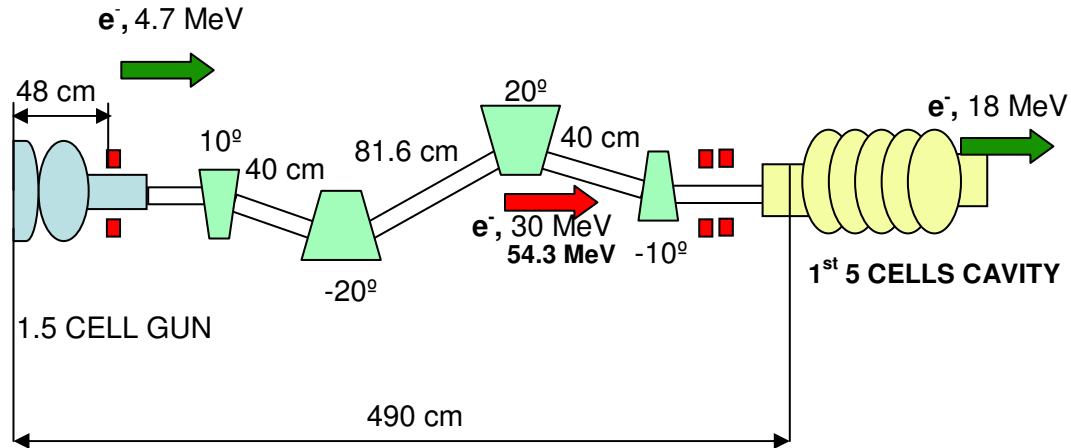


Figure VI-1. Schematic layout of SC RF Injector for the RHIC ERL electron cooler facility.

VI.A. SC RF GUN

The electron gun is required to produce a CW stream of electron bunches with a high charge (up to 5 nC), low emittance (below 4 microns normalized rms) and a high repetition rate (9.383 MHz). The frequency of the gun will be 703.75 MHz, or the 75th harmonic of the 9.383 MHz bunch spacing frequency of RHIC II.

To operate in CW mode with 50 mA current and 4.7 MeV kinetic energy beam the gun should supply about 250 kW power in to the beam. Low RF power losses in superconducting RF (SRF) gun and high peak electric field near the cathode followed by emittance compensation schema make SRF guns ideal injectors for high current low emittance applications.

There are many different projects right now considering the use of SRF photo-injector. The first SRF gun developed with a successful insertion mechanism is Kernforschungszentrum Rossendorf (KFR) gun [3]. The gun operated successfully and demonstrated a peak electric field of 22 MV/m over the cathode area. It seems what in 3-4 years a SRF Gun will become a routine running injector for high current low emittances applications.

To keep the beam from the growing near the cathode a focusing element right at the cathode is very desirable. A cathode recess provides an electric RF focusing near a cathode region when an effect from the space charge force is the most significance. The 1½ cell gun shape with recess cathode is shown on Fig. VI-2. In result of the cathode recess the accelerating field at the cathode is reduced by factor of two (Fig. VI-3).

The performance of a SRF photo-injector has been studied using SUPERFISH (to calculate the electric and magnetic fields) by PARMELA [4] (to calculate the beam dynamics).

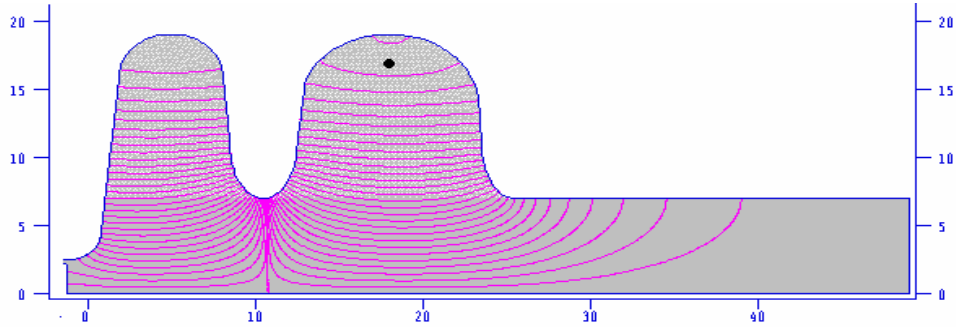


Figure VI-2. 1/2 cell gun model with recess cathode was used by SUPERFISH.

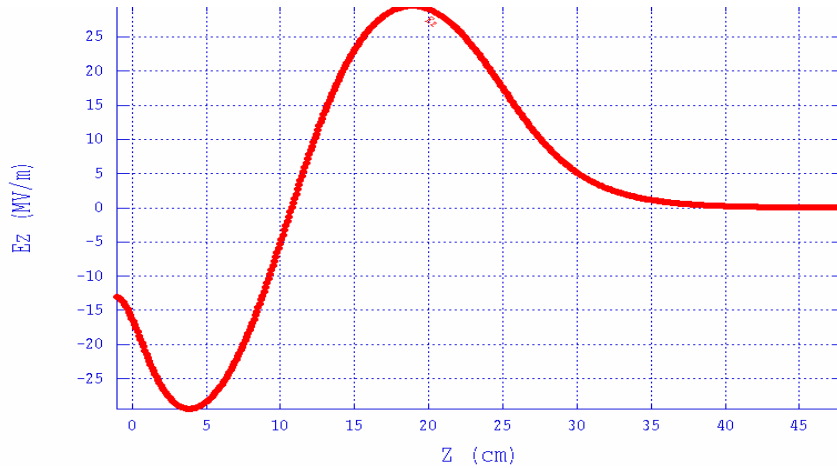


Figure VI-3. Electric field distribution for 1.5 cell gun calculated by SUPERFISH. One of an important part of running the gun is chosen correct launch phase. The analyze of energy gain dependence from the initial phase (Fig. VI-4) is shown what the crest point is setting at 42 degrees for this gun and this electric field. In order to minimize energy spread at the exit of the gun the 35 degrees launch phase is chosen [5].

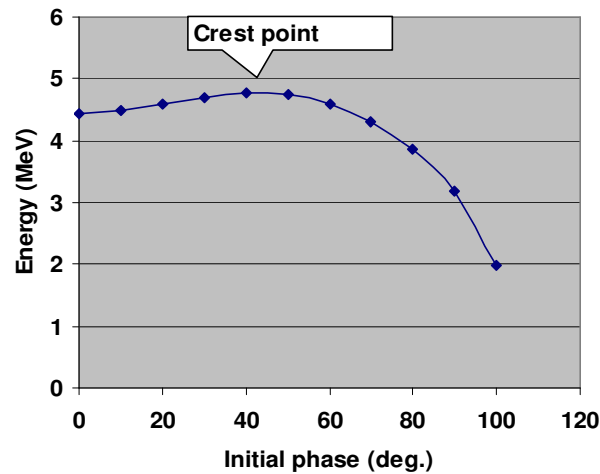


Figure VI-4. Energy gain from gun as a function of launch phase.

The longitudinal phase space at the exit of the gun is shown on Fig. VI-5. The parameters of the gun are presented in Tab.VI-1.

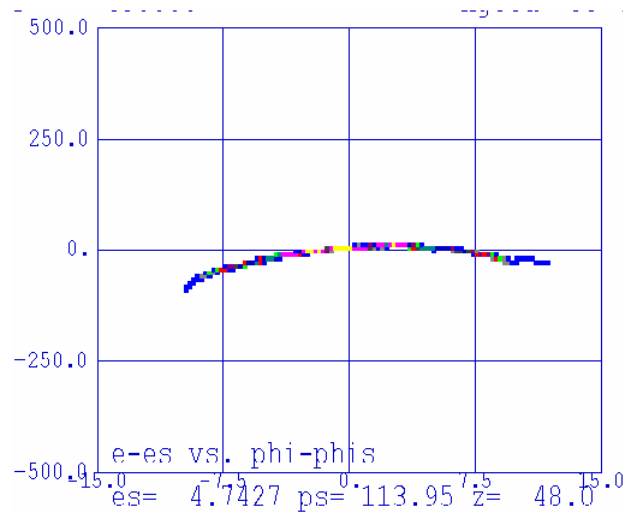


Figure VI-5. The longitudinal phase space after the gun for 5 nC electron bunch with elliptical initial distribution.

Table VI-1. 1½ cell SC Gun parameters

Frequency, MHz	703.75
Maximum field at the cathode , MV/m	14
Maximum electric field at the axis, MV/m	30
Maximum electric field at surface, MV/m	49.3
Maximum magnetic field at surface, A/m	76.8 kA/m
Initial phase, degrees	35
Charge/bunch, nC	5
Kinetic energy at the exit, MeV	4.7
Rms energy spread	6 3.2 10 ^{-3*})
Normalize emittance ex/ey, mm*mrad	7.6/7.6 ^{*)}

^{*)} Result for elliptical beam initial distribution: maximum radius 6.2 mm and maximum length 71 psec.

VI.B. MERGER SYSTEM

VI.B.1. Achromatic merger at present of a strong space charge effects

One of the critical parts of the injection line is the merger of the low energy- and high energy beams (Fig. VI-6). As the low energy beam is strongly affected by space charge the merge must be designed to minimize a degradation of the emittance. A typical system

of this type has two properly spaced focusing solenoids are used for the emittance compensation.

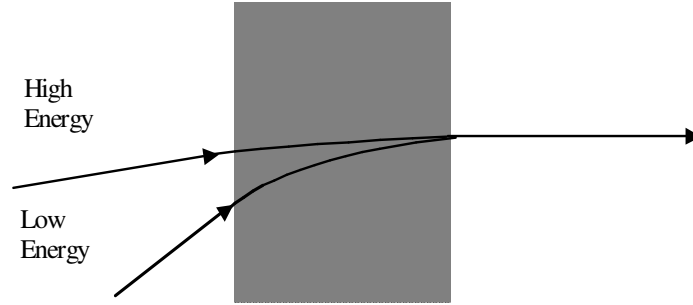


Figure VI-6. Main function of a merger – combining two (or more) beams with different energies

The injection energy is also the rest of the beam energy which is not recovered. To use low injection energy permits less power for gun and low dumped beam energy. The original emittance compensation schema [6] does not include any dipoles between RF gun and linac (or booster cavity). Focusing of the bending magnets in the merging section has significant effect on the low energy electrons. Different focusing in vertical and horizontal planes (astigmatism) requires different position of the linac which is impossible to obey. Hence, the use of chevron magnets with equal focusing strength in x- and y- direction is preferable. Any dipole magnet excites the coupling between energy and transverse motion which leads to effective correlated emittance growing:

$$\varepsilon_x^{eff} = \sqrt{\varepsilon_x^2 + \sigma_x^2 D'^2 \sigma_\delta^2 + \sigma_x'^2 D^2 \sigma_\delta^2},$$

where: D -is dispersion, D' -is dispersion derivative, ε_x is emittance without dispersion and $\sigma_x, \sigma_x', \sigma_\delta$ are rms size, angular spread and energy spread respectively.

The full merging system has to decouple such correlations at the exit (i.e. full decoupling longitudinal and transverse motions). There are many systems which work very well in zero approximation (no space charge effects and constant energy): chicane, dogleg, achromatic bend etc.

Basically it means that the achromatic system has to satisfy two traditional conditions:

$$\int_{s_0}^{s_f} K_0(s) \cdot m_{12}(s|s_f) \cdot ds = 0;$$

$$\int_{s_0}^{s_f} K_0(s) \cdot m_{22}(s|s_f) \cdot ds = 0,$$

where $K_0(s)$ -is curvature of trajectory, s_0, s, s_f - are initial, current and final positions respectively along the transport system $m_{12}(s|s_f), m_{22}(s|s_f)$ - are (1-2) and (2-2) elements of 6x6 transport matrix from s to s_f position.

In present strong space charge effect the particles energy is changing during the passing merger system. The additional two conditions have to be satisfied [7]:

$$\int_{s_0}^{s_f} K_o(s) \cdot s \cdot m_{12}(s|s_f) \cdot ds = 0;$$

$$\int_{s_0}^{s_f} K_o(s) \cdot s \cdot m_{22}(s|s_f) \cdot ds = 0.$$

One of the possible merging schemes which satisfied both pairs of conditions and preserves the emittance of the low energy is shown in Fig. VI.7. This system provides a minimum set of elements (4 magnets) for correlations compensation. The beauty of zigzag system is demonstrated in Fig.VI-8 where three different merger systems are compared. The vertical emittances for zigzag merger, chicane and simple straight line with solenoids focusing instead of dipole focusing are the same. That illustrates what the effective focusing in these three systems is similar. But only for zigzag system horizontal emittance (direction where the dispersion is excited) equal vertical one. The weak enough focusing by dipoles in this system is well compatible with emittance compensation technique where assumed that electrons are moving laminar (i.e. electron trajectories do not cross) [5]. For dogleg system because of strong focusing is implemented there is no laminar electrons moving any more. One of the important conditions for emittance compensation is broken. Even vertical emittance is much high than for straight line system.

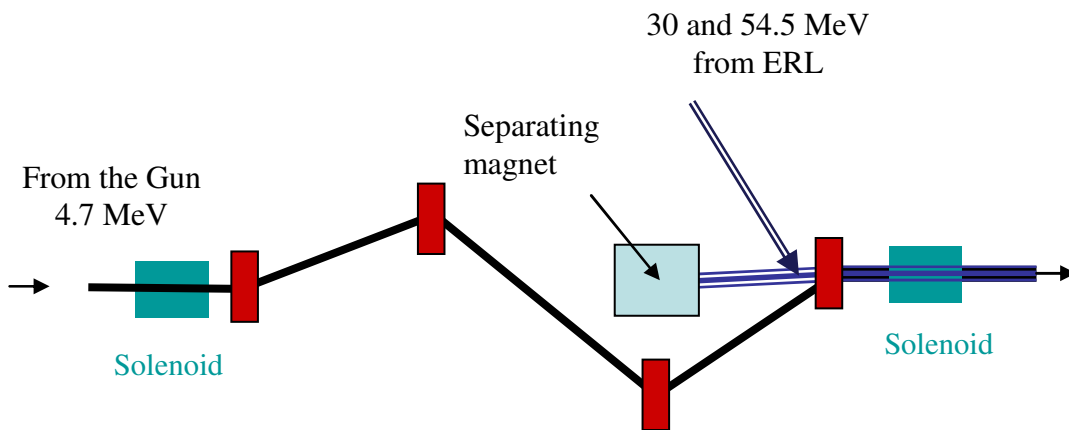


Figure VI-7. A merging system comprised of four chevron-type magnets, which is compensate the dispersion effects for space charge dominated beam.

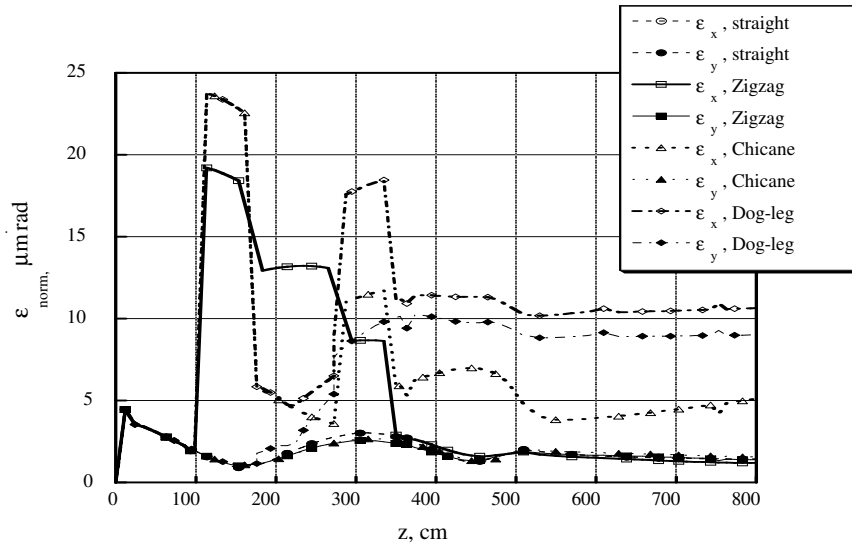


Figure VI-8. Evolution of horizontal and vertical normalized emittances in the four systems axially symmetric emittance compensation scheme, the Zigzag, the Chicane and the Dog-leg.

VI.B.2. Beam dynamic for different initial laser shape.

In order to get as better performance of the beam as possible three different types of laser driving pulse shapes were prepared (Fig. VI-9). All distributions are uniform in transverse direction and have different longitudinal distribution.

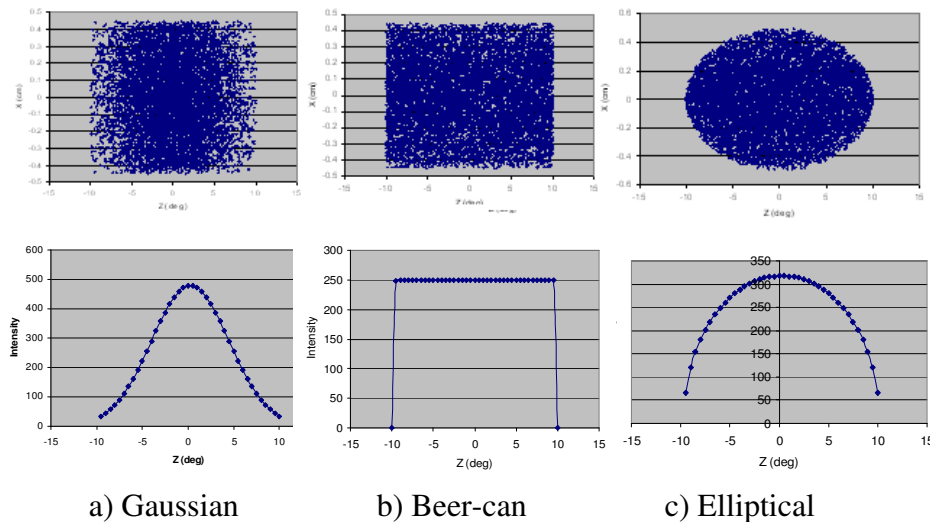


Figure VI-9. Three different initial laser shapes for beam dynamic simulation. First is Gaussian distribution which characterized by rms length 17 psec and radius 4.5 mm, second is so-called beer-can (or cylindrical) distribution characterized by full length 92 psec and radius 5.5 mm, the last one- elliptical distribution characterized by maximum radius 6.2 mm and maximum length 71 psec.

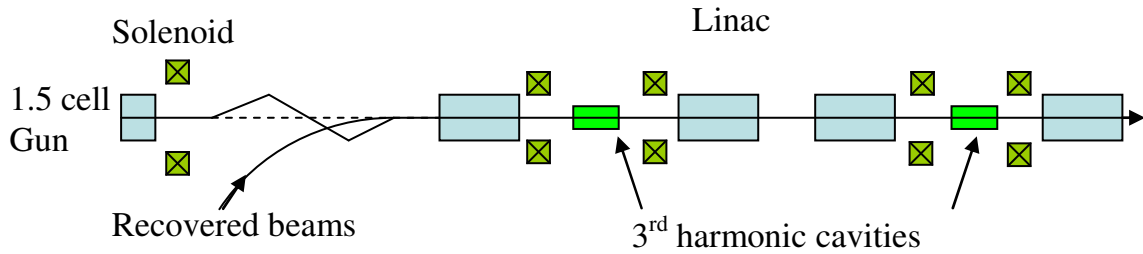


Figure VI-10. The test bed system for optimization injection part.

In order to save simulation time instead of running the beam through all ERL magnetic system the simple test-bed system was used. The test-bed system consist of the full scheme injector (for studies performance of which this test-bed was developed) followed by first pass through the linac and second time pass through the linac again without turning back loop between two passes (Fig. VI-10).

A normalized emittances evaluation in the test-bed system for beer-can initial distributions are shown on Fig. VI-11. The effective emittance jump because of dispersion exited by dipole magnet is well compensated by other dipole in the zigzag system. At the exit of the linac the horizontal normalized emittances is 3.1 mmrad and vertical is 2.8 mm mrad.

An energy spread evaluation is shown on Fig, VI-13, VI-14. Simulation result for three distributions is summarized in Tab. VI-2.

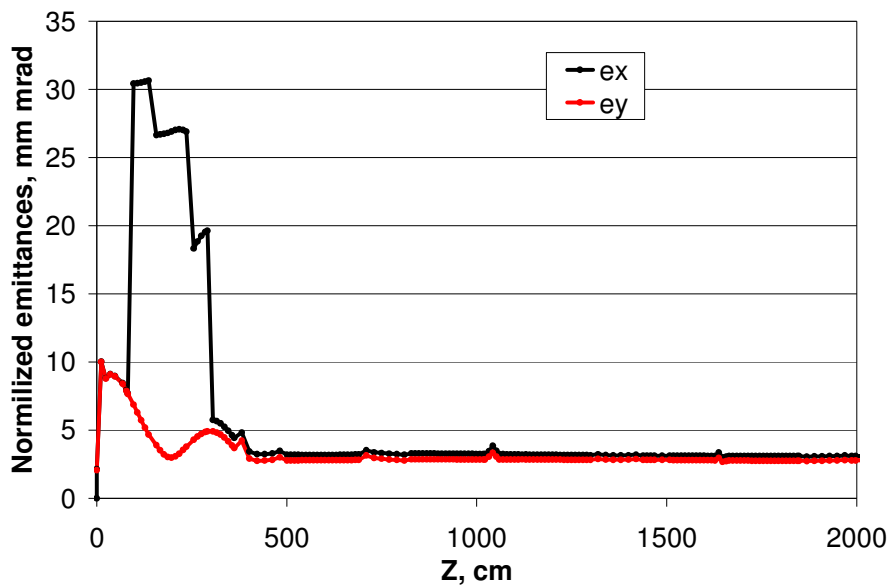


Figure VI-11. Normalized transverse emittances evaluation in test-bed system for beer-can distribution. (final horizontal emittance 3.1 mm mrad, vertical emittance 2.8 mm mrad)

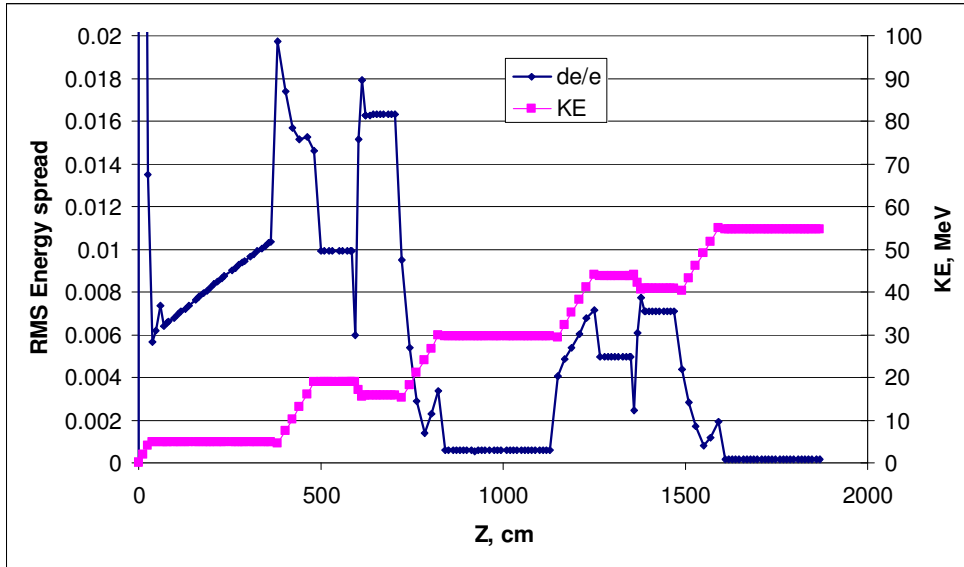


Figure VI-12. RMS energy spread and kinetic energy evolutions in test-bed system for beer-can distribution. (final energy spread $1.6 \cdot 10^{-4}$, kinetic energy 54.3 MeV)

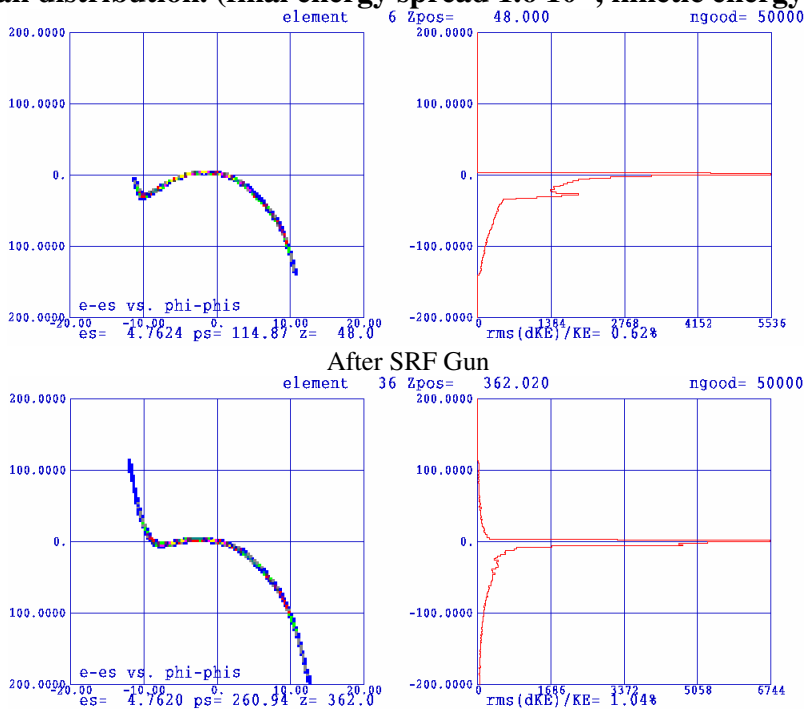


Figure VI-13. The longitudinal phase space at left side and energy spread at right at different locations (continued).

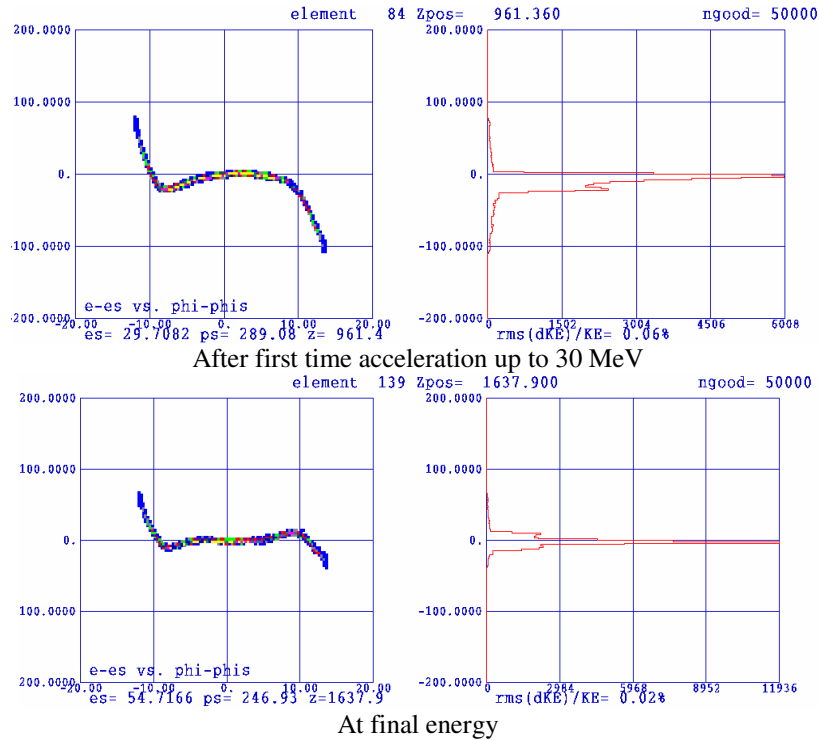


Figure VI-14. The longitudinal phase space at left side and energy spread at right at different locations (continued).

VI.B.3. Sensitivity to driving laser beam parameters.

Some aspects of sensitivity of final electron beam parameters to the initial laser pulse parameters were done. The results shows that for chosen launch phase and for beer-can distribution the electron beam parameters stay almost the same (Fig. VI-12).

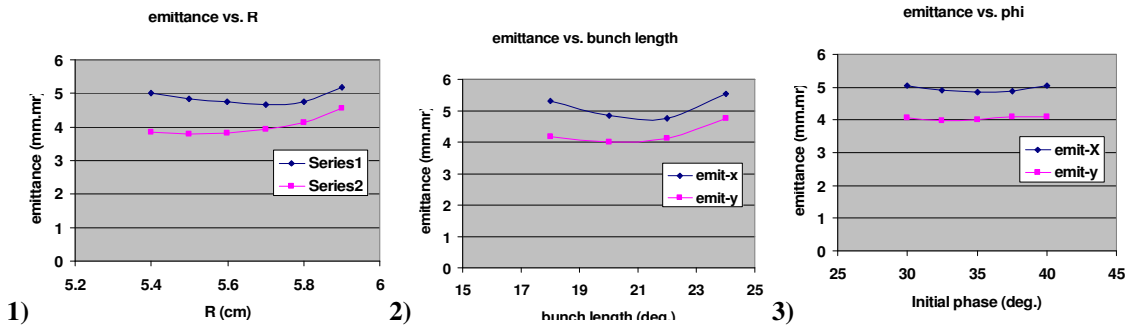


Figure VI-15. The dependence of final emittances from different laser beam parameters: 1) initial laser pulse length, 2) laser pulse radius, 3) laser launch phase

Table VI-2. The parameters of the electron beam at the exit of the test-bed system

	Gaussian	Beer-can	Elliptical
Kinetic energy , MeV	54.34	54.34	54.34
Charge per bunch, nC	5	5	5
Rms normalized emittance, ex/ey mm.mrad	5.9/4.6	3.2/2.9	3.0/2.4

Rms momentum spread	$4 \cdot 10^{-4}$	$1.8 \cdot 10^{-4}$	$2 \cdot 10^{-4}$
Rms bunch length, cm	0.58	0.78	0.54

VII. Start-to-end simulation.

Even for 55 MeV energy the space charge force can effect on the beam dynamic. For understanding that electron beam performance can be provided for electron cooling the electron beam is run using optics calculated by MAD8 (Fig. IV.A-2, Fig. IV.A-3).

Results of start to end simulation two passes ERL are shown in Fig. VII-1 and Fig. VII-2. Initial electron beam distribution is beer-can full length 92 psec and radius 5.5 mm. Beam parameters at the cooler work energy are shown in Tab. VII-1.

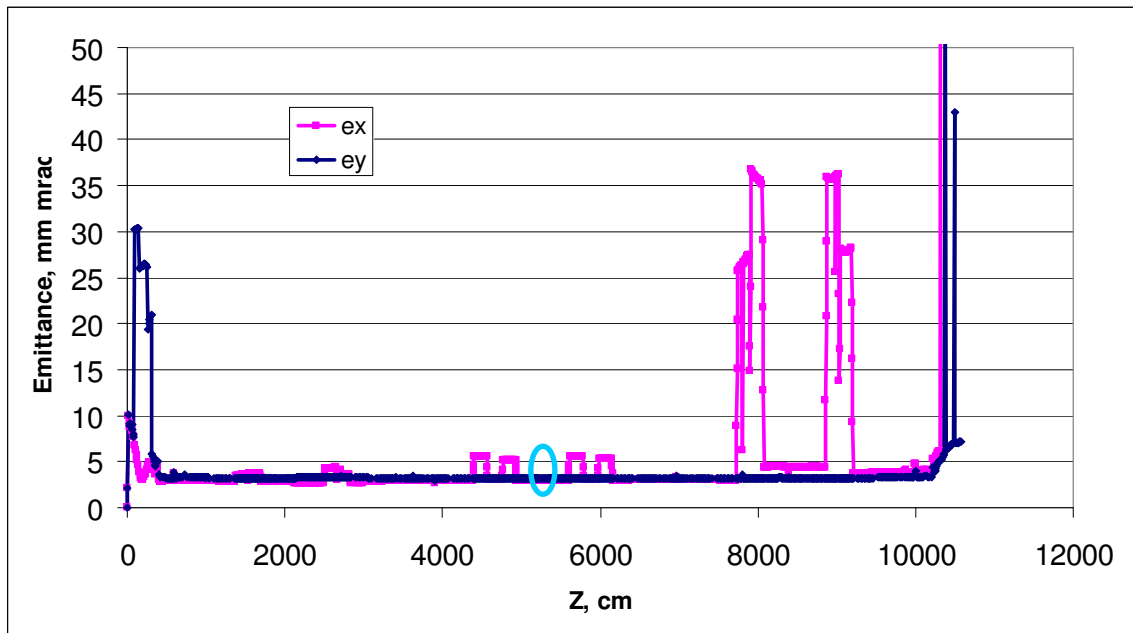


Figure VII-1. Normalized emittances evaluation in two passes ERL for electron cooler for beer-can distribution. ($ex/ey= 3.0/3.2$ mm mrad at kinetic energy 54.3 MeV). Cyan circle points location of the cooling section

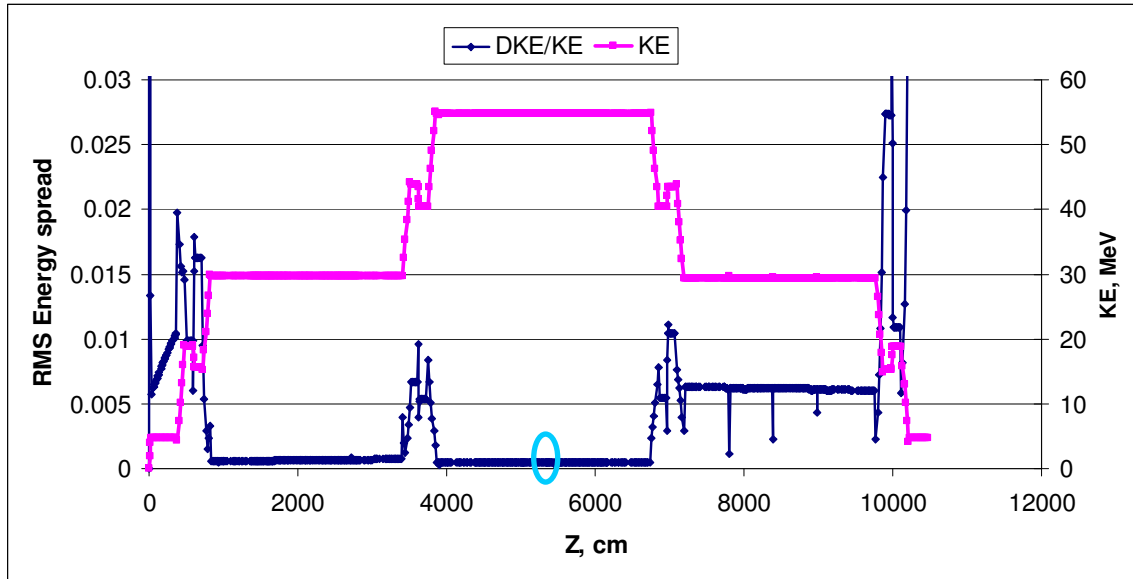


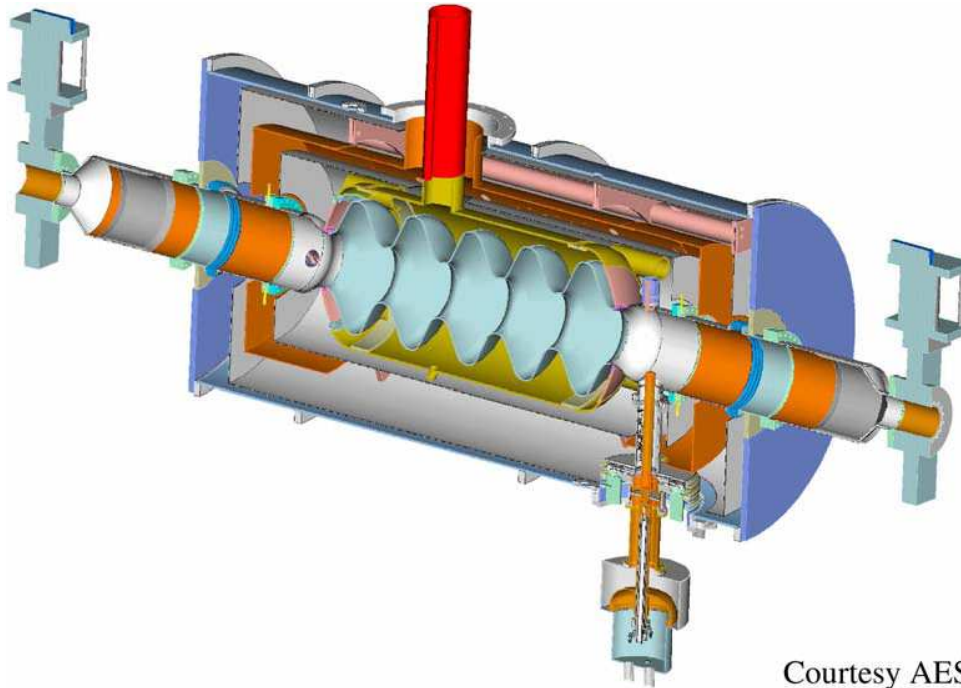
Figure VII-2. RMS energy spread and kinetic energy evolutions in two passes ERL for electron cooling for beer-can distribution. (energy spread $3.6 \cdot 10^{-4}$ at kinetic energy 54.3 MeV). Cyan circle points location of the cooling section

Table VII-1. The parameters of the electron beam at the working energy for electron cooling of gold ions.

Type of distribution	Beer-can
Kinetic energy, MeV	54.34
Charge per bunch, nC	5
Rms normalized emittance, ex/ey mm·mrad	3.0/3.2
Rms momentum spread	$3.6 \cdot 10^{-4}$
Rms bunch length, cm	0.78

VIII. Super conductive linac

The e-cooler linac has two 703.75 MHz SRF cavities equipped with effective HOM dumping system (Fig. VII-1) [8] and 3rd harmonic (2111 MHz) cavity between them. The rms bunch length is 1 cm or 8.4 degrees of 703.75 MHz.



Courtesy AES

Figure VIII-1. A 3-D view of the 5-cell SRF cavity design with complete cryomodule.

Because of the cosine dependence of the accelerating field, the off-crest electrons gain less than on-crest electrons. Hence, electron bunch has intrinsic energy spread, which is corrected by 2111 MHz SRF cavities. The third harmonic cavities are phased to decelerate the beam. The combined functions of the fundamental and 3rd harmonic cavities provide for increased range of uniform accelerating gain (Fig. VII-2).

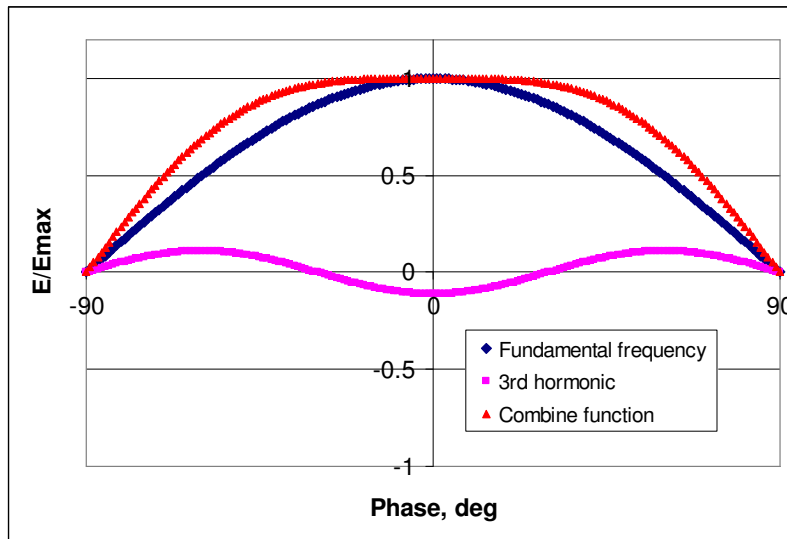


Figure VIII-2. Acceleration gain for different passing linac phase with and without 3-rd harmonic cavity.

The 703.75 MHz cavities will operate at 15 MV/m, the 2111 MHz cavities will operate at the gradient 8 MV/m. A resulting rms energy spread of the electron beam at the exit of

the linac because of cosine is $4 \cdot 10^{-4}$ (without 3rd harmonic cavity a rms energy spread due to cosine curvature is 10^{-2} , 25 times more).

It is important to notice that the 2111 MHz cavities should be located in the middle of the linac. Placing them at the end of the linac would create a problem: the beam would lose all energy during the deceleration in the 703.75 MHz cavities and would not reach the end of the beam dump. The HOM analysis of such super module has to be done.

The accelerating linac should be phased with the electron gun to accelerate the fresh beam during the first pass through it. The overall time lapse for the first loop should be equal to an even number of the RF cycles to be decelerated (the circumference should be about integer number of RF wavelengths).

IX. Beam break up instability

For high current ERL understanding of development beam break up instability is very important.

The transverse angular kick of the electron bunch in the cavity by the field of transverse HOM causes the displacement of the e-beam at the entrance of the cavity proportional to $m_{1,2}$ element in the transport matrix after passing through the loop. If the HOM field excited by the displaced beam exceeds the loss of the field caused by the HOM dumping, the beam became unstable.

One of the main futures of the of the 5 cell SC cavity developed BNL and AES is very low quality factors for HOMs. This is result of enlargement entrance/exit pipe and putting ferrate absorber in proper location.

From Eduard Pozdeyev (Jefferson Lab) studies of the two loops ERL with two 5 Cell cavities the threshold average current is always more than 1.5 A. Which is sufficiently for e-cooling operation: average current 0.05 A. But more studies including 3rd harmonic cavity have to be done.

REFERENCES

- [1] Electron Cooling for RHIC, I. Ben-Zvi, et al., Proceedings of the 2001 Particle Accelerator Conference, Chicago, IL, USA, June 18-22, 2001, p.48
- [2] A. Fedotov "Electron Cooling studies for RHIC-II"
http://www.bnl.gov/cad/ecooling/docs/PDF/Electron_Cooling.pdf
- [3] D.Janssen et al., NIM A, 507 (2003) pp 314-317.
- [4] Xiangyun Chang, Ilan Ben-Zvi, and Jörg Kewisch, "Emittance compensation of compact superconducting guns and booster linac system", Phys. Rev. ST Accel. Beams 9, 044201 (2006). <http://prst-ab.aps.org/abstract/PRSTAB/v9/i4/e044201>
- [5] L. M. Young, J. H. Billen, "Parmela documentation", LA-UR-96-1835.
- [6] L. Serafini and J. B. Rosenzweig, Phys. Rev. E 55, 7565 (1997).
- [7] V.N. Litvinenko, R. Hajima, D. Kayran, "Merger designs for ERL". NIM A 557, (2006) pp 165-175.
- [8] R. Calaga et al., "High Current Superconducting Cavities at RHIC", TUPKF078, Proceedings of EPAC-2004, Geneva, Switzerland, July 5-9, 2004